The Journal of Experimental Biology 209, 1803-1815
Published by The Company of Biologists 2006
doi:10.1242/jeb.02202

Transcriptional regulation of neuropeptide and peptide hormone expression by the *Drosophila dimmed* and *cryptocephal* genes

Sebastien A. Gauthier[1,*] and Randall S. Hewes[1,2]

[1]*Department of Zoology, Stephenson Research and Technology Center, University of Oklahoma, Norman, OK 73019, USA and* [2]*Department of Cell Biology, University of Oklahoma Health Sciences Center, Oklahoma City, OK 73104, USA*

*Author for correspondence (e-mail: seb-usa@ou.edu)

Accepted 4 March 2006

Summary

The regulation of neuropeptide and peptide hormone gene expression is essential for the development and function of neuroendocrine cells in integrated physiological networks. In insects, a decline in circulating ecdysteroids triggers the activation of a neuroendocrine system to stimulate ecdysis, the behaviors used to shed the old cuticle at the culmination of each molt. Here we show that two evolutionarily conserved transcription factor genes, the basic helix-loop-helix (bHLH) gene *dimmed* (*dimm*) and the basic-leucine zipper (bZIP) gene *cryptocephal* (*crc*), control expression of diverse neuropeptides and peptide hormones in *Drosophila*. Central nervous system expression of three neuropeptide genes, *Dromyosuppressin*, *FMRFamide-related* and *Leucokinin*, is activated by *dimm*. Expression of *Ecdysis triggering hormone* (*ETH*) in the endocrine Inka cells requires *crc*; homozygous *crc* mutant larvae display markedly reduced *ETH* levels and corresponding defects in ecdysis. *crc* activates *ETH* expression though a 382 bp enhancer, which completely recapitulates the *ETH* expression pattern. The enhancer contains two evolutionarily conserved regions, and both are imperfect matches to recognition elements for activating transcription factor-4 (ATF-4), the vertebrate ortholog of the CRC protein and an important intermediate in cellular responses to endoplasmic reticulum stress. These regions also contain a putative ecdysteroid response element and a predicted binding site for the products of the *E74* ecdysone response gene. These results suggest that convergence between ATF-related signaling and an important intracellular steroid response pathway may contribute to the neuroendocrine regulation of insect molting.

Supplementary material available online at
http://jeb.biologists.org/cgi/content/full/209/10/1803/DC1

Key words: bHLH, bZIP, *Drosophila*, ecdysis, stress, ETH.

Introduction

Neuropeptides and peptide hormones are small chemical transmitters that carry physiological messages to the attention of specific target cells. They are present in vertebrates and invertebrates and control diverse processes, including growth, stress responses, reproduction, homeostasis and memory (Nässel, 2002; Strand, 1999). A central feature of neuroendocrine signaling is the regulation of the synthesis and secretion of neuropeptides by inputs to neurosecretory cell afferents (Burbach, 2002). In many systems, the mechanisms regulating neuropeptide expression and secretion, and the genes and cell signaling pathways underlying these processes, are largely unknown.

The *Drosophila melanogaster dimm* gene encodes a bHLH protein (DIMM) in the Atonal family of transcription factors (Hewes et al., 2003). This family includes NeuroD, Neurogenin, Mist1 and Olig, which play essential roles in the determination and execution of cell fate decisions in many tissues (Hassan and Bellen, 2000). Likewise, DIMM determines secretory protein levels in diverse neuropeptidergic cells. The *dimm* gene is highly expressed in neuroendocrine cells, and *dimm* mutant animals display strikingly reduced cellular levels of various neuropeptides, neuropeptide biosynthetic enzymes (Hewes et al., 2003) and a dopamine receptor (Park et al., 2004). In contrast, *dimm* mutations do not disrupt cell survival or the differentiation of neuropeptidergic cell types, and the functions of *dimm* are largely restricted to development of the neuropeptide secretory pathway (Hewes et al., 2003). Does *dimm* regulate the expression of other transcription factors or structural proteins required for secretory granule biosynthesis, or does *dimm* directly regulate the expression of many secretory proteins?

In the present study we examined whether *dimm* is required for normal expression of neuroendocrine genes. We monitored

16 genes encoding neuropeptides, peptide hormones, neuropeptide biosynthetic enzymes, secretory granule proteins, and enzymes involved in synthesis of biogenic amines. Levels of these transcripts in *dimm* mutants and in control genotypes were measured by quantitative real-time polymerase chain reaction (qRTPCR) and *in situ* hybridization. To disrupt *dimm* expression, we used several genetic aberrations that differentially disrupt *dimm* and/or a neighboring gene, *crc*. *crc* encodes a basic-leucine zipper (bZIP) transcription factor that is orthologous to activating transcription factor-4, ATF-4 (Hewes et al., 2000), an important mediator of the unfolded protein response to endoplasmic reticulum stress (Blais et al., 2004). We have previously tested several *crc* alleles (crc^1, crc^{E98}, crc^{929} and *Df(2L)TW1*) by immunostaining with anti-neuropeptide antisera (myomodulin and –RFamide) and anti-neuropeptide biosynthetic enzyme antisera (Furin 1 and Amontillado), and in each case, the levels of these markers were unaffected by disruption of *crc* (Hewes et al., 2003; R.S.H., unpublished). Therefore, we predicted that secretory protein mRNAs would be found at normal levels in crc^1/crc^1 larvae, and we included this genotype as a control for the qRTPCR experiments.

Levels of three neuropeptide mRNAs, *Dromyosuppressin* (*Dms*), *FMRFamide-related* (*Fmrf*) and *Leucokinin* (*Lk*), were all reduced by disruption of *dimm* and not *crc*. However, *crc* was required for expression of the *ETH* gene in the endocrine Inka cells. Comparative genome sequence analysis revealed putative recognition elements in the *ETH* promoter for factors in the ecdysteroid response pathway and CRC. Our results suggest that DIMM controls the transcription of multiple neuroendocrine genes. Additionally, the molting defects in animals bearing the crc^1 mutation, a classical allele first discovered in 1942 (Hadorn and Gloor, 1943), result from loss of a key endocrine regulator of ecdysis behavior.

Materials and methods

Fly strains and genetic manipulations

Drosophila melanogaster Meigen stocks were cultured on standard cornmeal–yeast–agar media at 22–25°C. The following alleles were used to disrupt genes in the 39D1 region of chromosome 2L (Fig. 1, Table 1, and Table S2 in the supplementary material): *Df(2L)Rev8* (*Rev8*), *Df(2L)Rev4* (*Rev4*) and crc^1 (Hewes et al., 2000); *P{SUPor-P}*$dimm^{KG02598}$ ($dimm^{KG02598}$) (Hewes et al., 2003); and *P{EPgy2}*$dimm^{EY14636}$ (Bellen et al., 2004). The *ETH-EGFP* reporter line (Park et al., 2002) was kindly provided by Michael Adams (University of California, Riverside). Mutations were balanced over *CyO-y*$^+$ or *CyO, P{Ubi-GFP.S65T}PAD1* (*CyO, Ubi-GFP*). Oregon-R was used as the wild-type strain.

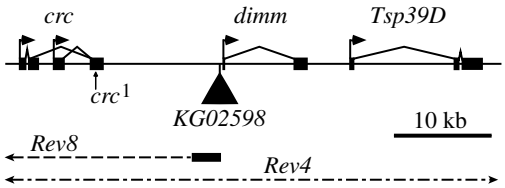

Fig. 1. Genomic map of the 39D1 region, showing the locations of three genes (*crc*, *dimm* and *Tsp39D*), the *P* element insertion in $dimm^{KG02598}$ (arrowhead), a single non-conservative base substitution in the crc^1 allele, and two local deletions (*Rev8* and *Rev4*). The box on *Rev8* indicates the proximal breakpoint uncertainty region.

RNA extraction

RNA extractions were performed on 24.5°C collections of 50 hatchling larvae on apple juice–agar plates supplemented with yeast paste. At this stage, the central nervous system (CNS) fills approximately 20–30% of the total body volume. The CNS volume:body volume ratio decreases with larval growth, and early collections maximized the relative yield of CNS mRNAs that could be obtained from whole animals. In addition, several of the neuropeptide transcripts measured in this study are expressed exclusively or primarily in the CNS (e.g. *Fmrf* and *Dms*) (Nichols, 2003; Schneider et al., 1991). Larval genotypes were distinguished by scoring for *yellow* (*y*) or *UBI-GFP*.

Tissues were disrupted by Polytron homogenization (Brinkmann, Westbury, NY, USA) on speed 5 for 5 min on ice. Total RNA was extracted in Trizol (Invitrogen, Carlsbad, CA, USA), in two extractions separated by a DNase treatment (RQ1 DNase kit; Promega, Madison, WI, USA). We synthesized cDNA from total RNA using random hexamer primers with the ISCRIPT kit (Bio-Rad, Hercules, CA, USA). One complete reaction and one 'No Enzyme' (NoE) reaction was performed for each RNA sample, with 50 ng (by spectrophotometry) of total RNA per reaction (reverse transcriptase was omitted from the NoE reactions).

qRTPCR

Three sets of PCR primers were designed using Primer3 (Rozen and Skaletsky, 2000) for each gene in our analysis (Table 2). Based on product quality and purity using genomic DNA templates (judged by the presence of a single band of the correct size in 2% agarose electrophoresis gels and by the homogeneity of amplicon T_m values in qRTPCR dissociation

Table 1. *Paired genotype comparisons used in the qRTPCR analysis*

Allele	Allele class	Control genotype	Test genotype
Rev8	Null *crc* allele and strong *dimm* hypomorph	*yw; Rev8/CyO, y+*	*yw; Rev8/Rev8*
$dimm^{KG02598}$	Weak *crc* allele and strong *dimm* hypomorph	*yw;* $dimm^{KG02598}$*/+*	*yw;* $dimm^{KG02598}$*/Rev4*
Rev4	Null allele for *crc*, *dimm* and *Tsp39D*		
crc^1	Strong *crc* hypomorph	*yw;* crc^1*/CyO, y+*	*yw;* crc^1/crc^1

Table 2. *Genes selected for qRTPCR analysis*

Category	Gene	Known or predicted function(s)	Protein levels in *dimm*$^{-/-}$ mutants
Neuropeptide biosynthetic enzymes	*Furin 1* (*Fur1*)	Neuropeptide endoprotease (Roebroek et al., 1991)	Reduced[a]
	Peptidylglycine-α-hydroxylating monooxygenase (*Phm*)	Neuropeptide amidation (Jiang et al., 2000)	Reduced[a]
	amontillado (*amon*)	Neuropeptide endoprotease (PC2) (Siekhaus and Fuller, 1999)	Reduced[b]
Secretory granule proteins	*ia2*	Protein tyrosine phosphatase (Walchli et al., 2000)	ND
	Calcium activated protein for secretion (*Caps*)	Secretory granule protein (Renden et al., 2001)	ND
dimm region	*dimmed* (*dimm*)	bHLH transcription factor[a]	ND
	cryptocephal (*crc*)	bZIP transcription factor (Hewes et al., 2000)	ND
	Tetraspanin 39D (*Tsp39D*)	Tetraspanin (Todres et al., 2000)	ND
Neuropeptides	*Pigment–dispersing factor* (*Pdf*)	Neuropeptide[f]	Normal[a,c]
	FMRFamide-related (*Fmrf*)	Neuropeptide[f]	Reduced[a]
	Dromyosuppressin (*Dms*)	Neuropeptide[f]	Reduced[a,d]
	Drososulfakinin (*Dsk*)	Neuropeptide[f]	Reduced[a,d]
	Leucokinin (*Lk*)	Neuropeptide[f]	Reduced[a]
	Cardioacceleratory peptide (*Ccap*)	Neuropeptide[f]	ND
	Eclosion hormone (*Eh*)	Neuropeptide[f]	Normal[a]
	Ecdysis triggering hormone (*ETH*)	Peptide hormones (ETH1 and ETH2)[f]	Reduced[a,e]
Biogenic amine synthetic enzymes	*Dopa decarboxylase* (*Ddc*)	Dopa decarboxylase (Livingstone and Tempel, 1983)	Normal[a]
	pale (*ple*)	Tyrosine hydroxylase (Neckameyer and White, 1993)	ND
Ribosomal	*Ribosomal protein L32* (*RpL32*)	Ribosomal protein (O'Connell and Rosbash, 1984)	ND

[a](Hewes et al., 2003)
[b](Park et al., 2004)
[c]Native expression pattern only.
[d]Inferred from immunostaining of the MP1 and MP2 neurons with the PT-2 antiserum, which detects –RFamide-containing peptides (Taghert, 1999), likely including DMS and DSK. The MP1 cells express *Dsk*, and the MP2 cells are immunopositive for DMS (Nichols et al., 1997).
[e]Inferred from immunostaining of the endocrine Inka cells with the anti-myomodulin (MM) antiserum (Hewes et al., 2003). This antiserum likely cross-reacts with ETH, since both peptides share a PRL-amide C-terminal motif (Zitnan et al., 2003).
[f]For reviews see (Hewes and Taghert, 2001; Vanden Broeck, 2001).
ND, not done.

curves), the best pair of primers was then selected (see Table S1 in the supplementary material). Primer concentrations were picked according to the nearest neighbor thermodynamic parameters method with salt corrections (SantaLucia, Jr, 1998) to match the conditions of the ABI qRTPCR cycle protocol (50 cycles: 15 s at 95°C followed by 1 min at 60°C on an ABI 7000; Applied Biosystems, Foster City, CA, USA).

Gene-specific qRTPCR reactions were performed with 1 μl of the reverse transcriptase mix, a pair of gene-specific primers, and SYBR green dye (ABI SYBR green PCR master mix). Each qRTPCR run was performed on a 96-well plate, providing transcript level information for 11 genes and the *Ribosomal protein L32* (*RpL32*) control (see below) for two experimentally paired genotypes. For each gene on the plate, we performed three technical qRTPCR replicates per genotype and one 'No Template' (NoT) reaction. NoT reactions lacked cDNA and were used to detect potential template-independent PCR amplification. For each genotype, we included two technical replicates with the *RpL32* primer set and the NoE control to check for potential genomic DNA contamination. In all cases, PCR products in NoE and NoT reactions were at least 50-fold less concentrated than the gene-specific qRTPCR products. Thus, contamination with genomic DNA and primer-related templates was negligible. In addition, melting temperatures of the gene-specific amplicons were always consistent across the technical and biological replicates and across all genotypes (data not shown).

We performed relative quantitation analysis on qRTPCR data using the housekeeping gene, *RpL32* (*rp49*), as a control. Levels of *RpL32* mRNA were not significantly different between paired genotypes (data not shown) and were therefore

not affected by mutations in the *dimm* region. For each PCR reaction, we obtained a Ct value representing the number of PCR cycles necessary to reach a threshold amplicon concentration. Ct values were normalized to *RpL32* to obtain ΔCt values ($\Delta Ct=Ct_{test\ gene}-Ct_{RpL32}$), which were then averaged across the three technical replicates. By comparing levels of each transcript to *RpL32*, we confirmed consistency of the mRNA extraction, cDNA synthesis, and loading for the two paired genotypes within each experiment. In addition, normalization of test gene Ct values to those of *RpL32* allowed us to compare transcript levels across experiments.

Tissue preparation and image analysis

Anti-*Manduca* pre-ecdysis triggering hormone (anti-PETH) immunostaining (Park et al., 2002; Zitnan et al., 1999) and *ETH-EGFP* imaging, preparation of digoxigenin-labeled DNA probes (from genomic templates), and whole-mount larval or CNS *in situ* hybridization were performed as described (Hewes et al., 2003). Control and experimental genotypes were always processed in parallel within a given experiment, using the same reagents, to minimize variability. In addition, for the *in situ* hybridization analysis, all reactions were stopped at the same time (when the most intense signals first became dark to prevent overstaining). We then measured the intensity of each cellular signal (intensity index) as described (Hewes at al., 2003). Briefly, confocal (fluorescence) and CCD (brightfield) images were obtained after adjusting exposure settings to optimize detection without saturating the signal. For a given neuron, identical settings were used for all preparations and genotypes, and the mean pixel intensity for the area covering each soma (S), and the neighboring background (B), was measured using Adobe Photoshop (San Jose, CA, USA). The intensity index=(S–B)/B. Images shown in the figures were chosen to best represent the mean intensity index values.

Statistical analysis

Statistical analyses were performed using NCSS 2001 (Kaysville, UT, USA). Sequential Bonferroni corrections were performed to minimize type I errors in multiple pair-wise comparisons (Rice, 1989). We used parametric statistics, because the data generally followed a normal distribution. All values are means ± s.e.m.

Comparative genomic analysis of the 382 bp ETH regulatory region

Drosophila genome sequences were visualized with VISTA (VGB2.0) (Frazer et al., 2004), using AVID and SLAGAN alignments, on the UCSC Genome Browser at http://genome.ucsc.edu/ (Karolchik et al., 2003) and with the MAVID multiple alignment server at http://baboon.math.berkeley.edu/mavid/ (Bray and Pachter, 2004). The alignments included sequences from eight *Drosophila* genomes: *D. melanogaster* (January 2003 assembly) (Celniker et al., 2002); *D. pseudoobscura* (July 2003) (Richards et al., 2005); *D. yakuba* (April 2004) and *D. simulans* (December 2004; Genome Sequencing Center, Washington University School of Medicine); *D. ananassae* (July 2004; The Institute for Genomic Research); *D. mojavensis* (August 2004), *D. erecta* (October 2004) and *D. virilis* (July 2004; Agencourt Bioscience Corporation). Consensus sequences (IUPAC code) were obtained using the TRANSFAC (see below) adaptations of the Cavener rules (Cavener, 1987). The code was capitalized when the nucleotide was present in at least seven sequences in the eight-species alignment.

The conservation track (phastCons) in the UCSC Genome Browser was based on a MULTIZ alignment of the *D. melanogaster*, *D. yakuba* and *D. pseudoobscura* genomes. These scores present an estimate of evolutionary conservation based on phylogeny, nucleotide substitution rates and autocorrelation of conservation levels along the genome (Siepel and Haussler, 2005). Putative transcription factor binding sites were identified using rVISTA (Loots et al., 2002), using the TRANSFAC Professional 7.4 library of binding site sequences (BIOBASE Biological Databases, Wolfenbüttel, Germany).

Results

Differential effects of aberrations in 39D1 on dimm, crc and Tsp39D expression

We used qRTPCR to analyze neuropeptide gene expression because of the sensitivity of this method. This was true even with whole-animal RNA samples, because a large majority of the cells that express *dimm*-dependent neuroendocrine peptides in our analysis (e.g. the populations of cells that express LK and ETH; Table 2) are affected in *dimm* mutant animals (Hewes et al., 2003). Based on our earlier immunocytochemical studies, we chose the neuropeptide and peptide biosynthetic enzyme genes for this analysis based on whether they were expressed in patterns largely or completely overlapping with *dimm*, and whether they showed reductions in protein levels in *dimm* mutant larvae (Hewes et al., 2003). However, we also included neuropeptide genes (e.g. *Pdf*, *Eh*) encoding proteins that are known not to be affected in *dimm* mutants as internal controls.

Because all of the loss-of-function alleles of *dimm* were also loss-of-function alleles of the *crc* gene (Fig. 1), we used three different paired genotype comparisons, in order to reveal the effects of *dimm* specifically on levels of secretory protein mRNAs (Table 1). First, we performed qRTPCR to monitor transcript levels in *Rev8/Rev8* larvae and *Rev8/+* controls. The *Rev8* deletion is a null allele of *crc* and a strong loss-of-function allele of *dimm* (Hewes et al., 2003; Hewes et al., 2000). Second, we compared $dimm^{KG02598}$*/Rev4* mutants to $dimm^{KG02598}$*/+* controls. The *Rev4* deletion is a null mutation of both *crc* and *dimm*. In contrast, the $dimm^{KG02598}$ mutation is a strong *dimm* loss-of-function allele, but a weak loss-of-function allele of *crc* (Hewes et al., 2003). Therefore, in both of the first two experiments we tested the effects of double-mutant combinations of *dimm* and *crc*, but in the second experiment, the *crc* defects were much less severe. In the third experiment, we compared crc^{1}/crc^{1} larvae to crc^{1}/+ controls.

crc[1] is a strong *crc* loss-of-function allele, but it does not disrupt *dimm* (Hewes et al., 2003; Hewes et al., 2000).

We first examined the effects of the above genotypes on genes in the 39D1 region: *dimm* is flanked by *crc* and a second gene, *Tetraspanin 39D* (*Tsp39D*). As expected, *dimm* and *crc* transcript levels were reduced in *Rev8/Rev8* larvae (Fig. 2A). *Rev8* deletes the *crc* gene (Fig. 1), resulting in a dramatic decrease in *crc* mRNA levels (although some *crc* mRNA is maternally loaded) (Hewes et al., 2000). *Rev8/Rev8* mutants also display markedly reduced *dimm* mRNA levels (Hewes et al., 2003), presumably due to the deletion of *dimm* gene regulatory regions. In *dimm*^{KG02598}*/Rev4* mutants, levels of *crc*, *dimm* and *Tsp39D* transcripts were all lower than in the heterozygous controls (Fig. 2B). This result is consistent with our earlier observation that KG02598 is not only a strong hypomorphic allele of *dimm* but also a weak hypomorphic allele of *crc* (Hewes et al., 2003). We suspect that the broad effects of this insertion on genes in 39D1 are due to chromosomal insulator elements contained within the KG02598 element (Roseman et al., 1995). Finally, *dimm*, *crc*

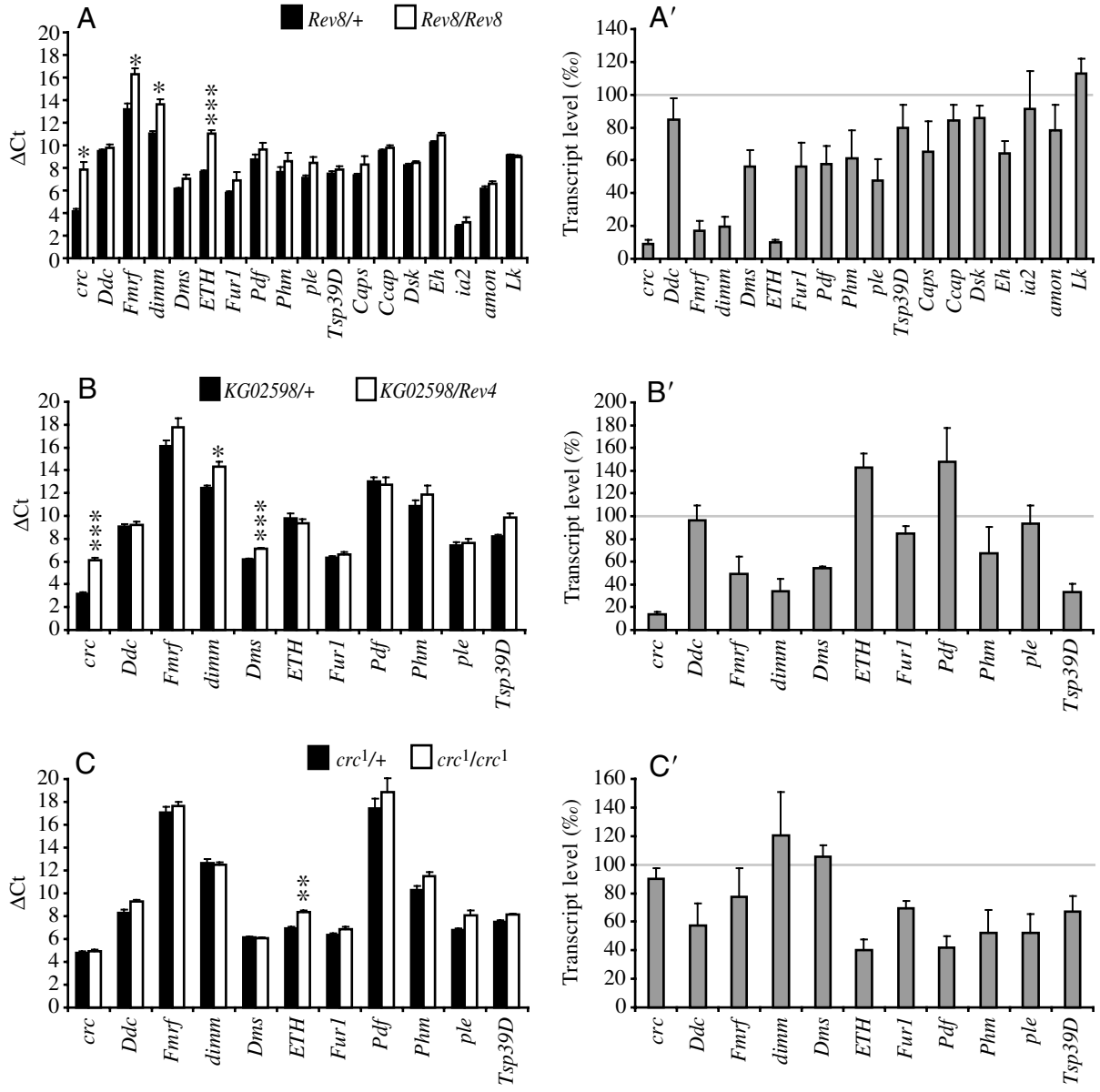

Fig. 2. Quantification of mRNA levels in hatchling larvae by qRTPCR. (A–C) Mean gene ΔCt values for (A) *Rev8/+ vs Rev8/Rev8* (*N*=5), (B) *dimm*^{KG02598}*/Rev4 vs dimm*^{KG02598}/+ (*N*=6) and (C) *crc*^{1}*/crc*^{1} *vs crc*^{1}/+ larvae (*N*=5). The *N* values represent the number of independent mRNA extractions. (A′–C′) Levels of transcripts in homozygous or transheterozygous mutants in A–C expressed as a percentage of the levels in heterozygous controls. During each cycle of the qRTPCR, the Ct value increases by 1 as the quantity of qRTPCR product is doubled. Therefore, the percentage change in each mRNA shown in A′–C′ was calculated as $1/2^{(\Delta Ct\ experimental - \Delta Ct\ control)}$. **P*<0.05; ***P*<0.01; ****P*<0.001; one-way ANOVA, sequential Bonferroni *post-hoc* test.

and *Tsp39D* transcript levels were not significantly different between crc^1/crc^1 and $crc^1/+$ (Fig. 2C). This result was expected because crc^1 is a missense mutation specific to *crc*, and because our earlier *crc in situ* hybridization analysis of crc^1/crc^1 animals showed no change in *crc* mRNA levels (Hewes et al., 2000). Thus, the levels of *dimm*, *crc* and *Tsp39D* transcripts behaved as predicted in the three qRTPCR experiments.

Three neuropeptide transcripts are downregulated in dimm and crc mutants

Only three neuropeptide mRNAs, *Dms*, *Fmrf* and *ETH*, varied significantly between paired genotypes in at least one of the three qRTPCR experiments. *Dms* transcript levels were reduced by 46% in $dimm^{KG02598}/Rev4$ animals (Fig. 2B). Levels of *Dms* were also down by 44% in *Rev8/Rev8* mutants (Fig. 2A), although this difference was not statistically significant after the Bonferroni correction (P=0.047). In contrast, *Dms* transcript levels were normal in crc^1/crc^1 animals (Fig. 2C). We obtained similar results for *Fmrf*. *Fmrf* mRNA levels dropped 83% in *Rev8/Rev8* (Fig. 2A), and they were down 51% in $dimm^{KG02598}/Rev4$ (Fig. 2B), although the latter difference was not statistically significant (P=0.13). *Fmrf* transcript levels were normal in crc^1/crc^1 animals (Fig. 2C). Based on our *in situ* hybridization data (see below), the relatively low P values, and the conservative nature of the Bonferroni correction, it appears likely that the reductions of *Dms* in *Rev8/Rev8* and of *Fmrf* in $dimm^{KG02598}/Rev4$ were incorrectly judged as not significantly different due to type II error (false negatives). Notably, we previously observed reduced *in situ* hybridization with an *Fmrf* probe in $dimm^{KG02598}/Rev4$ larval CNS (Hewes et al., 2003). Therefore, the combined qRTPCR results suggested an effect of *dimm*, but not *crc*, on levels of *Dms* and *Fmrf* mRNA. These findings are consistent with the cellular reductions in immunocytochemical staining for the neuropeptide products of these two genes (Table 2).

The last of the three affected neuropeptide/peptide hormone mRNAs was *ETH*, which was reduced by 90% in the *Rev8/Rev8* mutants (Fig. 2A) and by 60% in the crc^1/crc^1 mutants (Fig. 2C). While the reduction in *ETH* levels caused by the *Rev8* chromosome was consistent with our previous studies (Table 2), the reduction in crc^1/crc^1 animals was novel, and we explored this relationship further (see below).

In the qRTPCR experiment comparing *Rev8/+* and *Rev8/Rev8*, we did not observe significant differences in transcript levels for three neuropeptide genes, *Pdf*, *Ccap* and *EH*, two genes that encode known or putative components of secretory granules in neuropeptidergic cells (*ia2* and *Caps*), and two genes, *Ddc* and *ple*, encoding enzymes involved in synthesis of biogenic amines (Fig. 2A). For *Pdf* and *Ddc*, these results are consistent with previous immunostaining data (Table 2). Thus, these seven transcripts were not affected by disruption of either *dimm* or *crc*, and we excluded them from the subsequent qRTPCR analysis of $dimm^{KG02598}/Rev4$ and crc^1/crc^1 (Fig. 2B,C).

Finally, there were five genes, *amon*, *Dsk*, *Fur1*, *Lk* and *Phm*, for which we observed no change in mRNA levels (Fig. 2) despite marked reductions in levels of their protein products (Table 2). In some cases, these differences may be due to indirect regulation of protein levels by *dimm*, such as through transcriptional regulation of other elements of the regulated secretory pathway (see Discussion).

dimm is required for normal Dms expression

The pattern of *in situ* hybridization with a *Dms* probe was similar to the reported immunostaining pattern (Nichols, 2003). *Dms* was expressed in ~14–16 cells, with one pair in the subesophageal region (SE) and at least three pairs in each brain lobe (LB, MP2 and SP) (Fig. 3A). Additional, faintly labeled cells were sometimes visible. In $dimm^{KG02598}/Rev4$ larval CNS, we observed significantly less signal in two cell types, SP and SE, than in the $dimm^{KG02598}/+$ controls (Fig. 3B). There was also a reduction in *Dms* levels in the MP2 cells, although this trend was not statistically significant. In contrast,

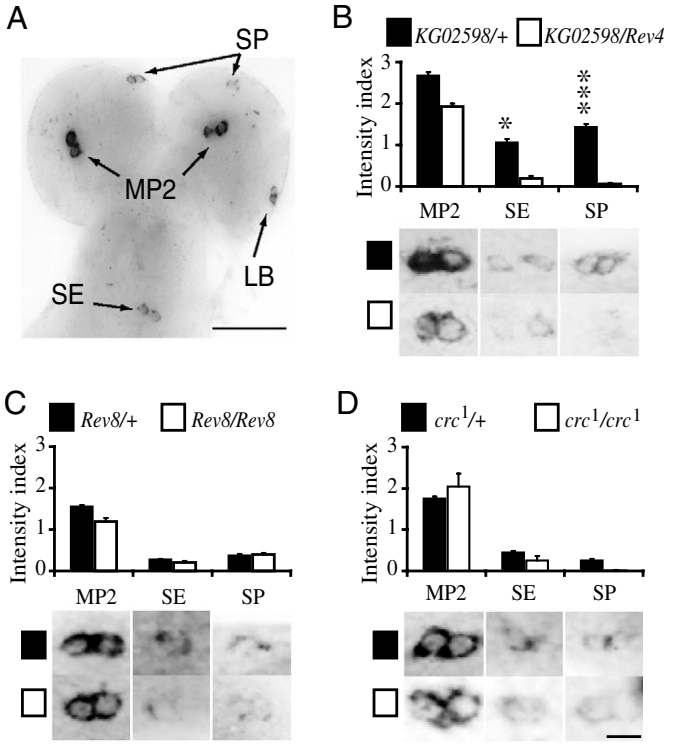

Fig. 3. Reduced *Dms* transcript levels in the CNS of *dimm* mutant, but not *crc* mutant, hatchling larvae. (A) *In situ* hybridization with a *Dms* antisense probe in $dimm^{KG02598}/+$ CNS. (B–D) Intensity of *Dms in situ* hybridization for the MP2, SE and SP cells in (B) $dimm^{KG02598}/Rev4$ (N=9) *vs* $dimm^{KG02598}/+$ (N=11), (C) *Rev8/Rev8* (N=12) *vs Rev8/+* (N=13), and (D) crc^1/crc^1 (N=5) *vs* $crc^1/+$ (N=11) larvae. Paired genotypes were processed for *in situ* hybridization in parallel within each experiment (e.g. *Rev8/Rev8 vs Rev8/+*) but not between experiments (e.g. B *vs* D), and the baseline *in situ* hybridization intensities between experiments cannot be directly compared. *P<0.05; ***P<0.001; one-way ANOVA. Scale bars: 25 μm (A); 2.5 μm (B–D).

we found no significant variation in the intensity of *Dms* hybridization between *Rev8/Rev8* and *Rev8/+* (Fig. 3C) or between crc^1/crc^1 and $crc^1/+$ (Fig. 3D). The reason for the effect of $dimm^{KG02598}$*/Rev4* but not *Rev8/Rev8* on *Dms* transcript levels is unclear, although $dimm^{KG02598}$ may simply be a stronger *dimm* allele than *Rev8*. However, these results are in general agreement with the qRTPCR data, and we conclude that *dimm*, and not *crc*, likely upregulates *Dms* gene expression and/or increases the stability of the *Dms* mRNA.

Lk neurons are differentially regulated by dimm

Previously, we found a marked reduction in levels of anti-LK immunostaining in *Rev8/Rev8* mutants (Hewes et al., 2003). The qRTPCR results here, however, showed no change in *Lk* transcript levels in *Rev8/Rev8* mutants, indicating that the regulation of LK protein levels in this genotype may be post-transcriptional. Therefore, we performed *Lk in situ* hybridization on *Rev8/Rev8* larvae to further test this hypothesis. In first instar larval CNS, we detected hybridization with an *Lk* antisense DNA probe in a pair of cells (Br1) in the brain lobes, in two pairs of cells in the subesophageal region (SE), and seven pairs of more weakly *Lk*-expressing cells (A1–A7) in the ventral nerve cord (VNC) (Fig. 4A). This pattern of expression appears to be identical to the immunostaining pattern (Hewes et al., 2003). In the A1–A7 cells of *Rev8/Rev8* mutant larvae, the strength of *Lk* hybridization was strongly reduced relative to *Rev8/+* controls (Fig. 4B). In contrast, levels of *Lk* in the SE and Br1 cells appeared to be increased in *Rev8/Rev8* animals, although the increase observed in the Br1 cells was not statistically significant. These results are consistent with our qRTPCR data, since increased *Lk* mRNA levels in the six Br1 and SE cells likely masked a decrease in *Lk* levels in the 14 more weakly *Lk*-expressing A1–A7 cells.

These cell type-specific changes in *Lk* mRNA levels also mirror our anti-LK immunostaining results. In multiple different $dimm^{-/-}$ genotypes, the A1–A7 cells display a greater reduction in anti-LK immunostaining than SE or Br1, although all three cell types are affected (data not shown). While we cannot exclude the possibility that *crc* regulates LK levels, the loss of *dimm* alone can account for these findings, since LK protein levels are also reduced by RNA interference directed against *dimm* (Hewes et al., 2003). These results show that in A1–A7, *dimm* likely upregulates *Lk* gene expression and/or increases the stability of the *Lk* mRNA. In SE and Br1, the responses are more complex, since *dimm* may downregulate *Lk* gene expression in these cells while increasing LK protein levels. Thus, in some cases, *dimm* may regulate neuropeptide synthesis at the transcriptional level as well as at a later step in the regulated secretory pathway (see Discussion).

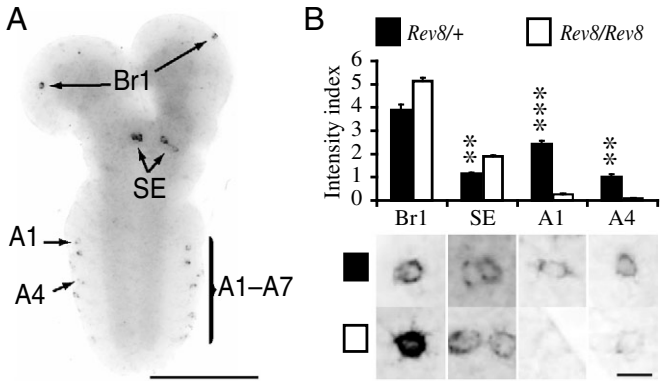

Fig. 4. Reduced *Lk* transcript levels in the CNS of *dimm*, *crc* double mutant hatchling larvae. (A) *In situ* hybridization with a *Lk* antisense probe in a wild-type CNS. (B) Intensity of *Lk in situ* hybridization for selected neurons in *Rev8/Rev8* (N=17) *vs* *Rev8/+* (N=12) larvae. $^{**}P<0.01$; $^{***}P<0.001$; one-way ANOVA. Scale bars: 50 μm (A); 2.5 μm (B).

crc regulates ETH expression

To further test the dependence of *ETH* levels on *crc*, we performed *in situ* hybridization with an *ETH* probe in *crc* mutant larvae. To facilitate preparation of larval fillets, we used third instar larvae, and we observed strong *ETH* hybridization in seven pairs of Inka cells (O'Brien and Taghert, 1998; Park et al., 2002). *ETH*-positive cells were located on the dorsal-longitudinal tracheal trunks in tracheal metameres 1 and 4–9 (TM1, TM4–TM9) (Manning and Krasnow, 1993). Compared to heterozygous controls, we found reduced *ETH* hybridization in $dimm^{KG02598}$*/Rev4* (Fig. 5A). The cause of the difference in the results for $dimm^{KG02598}$*/Rev4* in the qRTPCR *versus* the *in situ* hybridization analysis was not determined, but these experiments were performed on different larval stages, and the cumulative effects of $dimm^{KG02598}$*/Rev4* on *crc*-dependent processes may be more pronounced in older animals. Notably, *ETH in situ* hybridization was markedly reduced in crc^1/crc^1 larvae (Fig. 5B), consistent with the qRTPCR results (Fig. 2C). In addition, we observed a severe reduction in anti-PETH immunostaining (Park et al., 2002) in crc^1/crc^1 Inka cells (data not shown). This antiserum interacts with ETH-like peptides from diverse insect species (Zitnan et al., 2003), and it labels peptides in the *Drosophila* Inka cells that are presumably ETH1 and/or ETH2 (Park et al., 2002). These results provide strong additional evidence for an important role of *crc* in regulating *ETH* expression.

Does DIMM contribute to the regulation of ETH levels *in vivo* in addition to CRC? We have previously shown that *dimm* is expressed in the Inka cells (Hewes et al., 2003), but without a specific *dimm* mutant allele, this question could not be addressed directly. However, shortly before our completion of these experiments, the *Drosophila* Gene Disruption Project (Bellen et al., 2004) reported a *P* element insertion, *P{EPgy2}*$dimm^{EY14636}$ ($dimm^{EY14636}$), inserted in the *dimm* open reading frame in exon 2. To determine whether $dimm^{EY14636}$ disrupts *crc*, we performed lethal complementation analysis with other *dimm* and *crc* alleles (see Table S2 in the supplementary material). The $dimm^{EY14636}$ allele was semi-lethal (6–50% survival) in combination with *Rev4* and *Rev8*, and it was subvital (51–85% survival) over

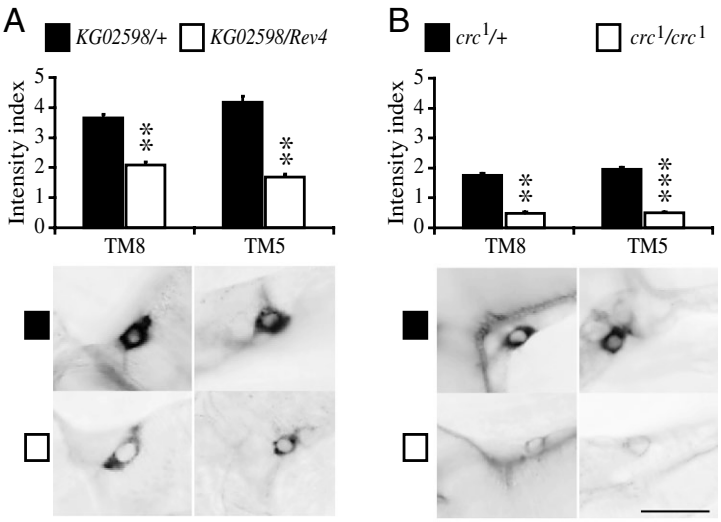

Fig. 5. Reduced *ETH* transcript levels in the endocrine Inka cells of *crc* mutant third instar larvae. (A,B) Intensity of *in situ* hybridization with an *ETH* antisense probe in the Inka cells on tracheal metameres 5 (TM5) and 8 (TM8) of the tracheae in (A) $dimm^{KG02598}$*/Rev4* (*N*=9) *vs* $dimm^{KG02598}$/+ (*N*=8) and (B) crc^1/crc^1 (*N*=9) *vs* crc^1/+ (*N*=10) larvae. ***P*<0.01; ****P*<0.001; one-way ANOVA. Scale bar, 10 μm.

$dimm^{KG02598}$. In contrast, $dimm^{EY14636}$ complemented crc^1. Therefore, $dimm^{EY14636}$ selectively disrupts *dimm* and not *crc*.

In $dimm^{EY14636}/dimm^{EY14636}$ larvae, we observed a marked reduction in CNS levels of anti-LK immunostaining relative to $dimm^{EY14636}$/+ controls (data not shown). We also observed a small decrease in the intensity of anti-PETH immunostaining in the Inka cells in $dimm^{EY14636}/dimm^{EY14636}$ larvae, although the strength of *ETH in situ* hybridization was unaffected (see Fig. S1 in the supplementary material). Thus, *crc* and *dimm* regulate *ETH* through distinct mechanisms. *crc* controls *ETH* transcription, whereas *dimm* can regulate ETH levels without altering *ETH* mRNA expression.

crc interacts with a 382 bp ETH regulatory region

Park et al. defined a 382 bp *ETH* enhancer region that is sufficient to direct expression of an *ETH-Enhanced green fluorescent protein* (*ETH-EGFP*) transgene specifically to the 14 Inka cells (Park et al., 2002). To determine whether this regulatory region is sensitive to regulation by *crc*, we monitored EGFP fluorescence in crc^1*/Rev4, ETH-EGFP* and $dimm^{KG02598}$*/Rev4, ETH-EGFP* third instar larvae. In $dimm^{KG02598}$*/Rev4, ETH-EGFP* CNS, we observed slightly reduced levels of EGFP relative to +/*Rev4, ETH-EGFP* controls (Fig. 6A), but this difference was not statistically significant (*P*=0.056, $Inka^{TM5}$; *P*=0.35, $Inka^{TM8}$). We observed a much stronger reduction in EGFP fluorescence in crc^1*/Rev4, ETH-EGFP* larvae (Fig. 6B). These findings, together with the qRTPCR and *in situ* hybridization results, demonstrate *crc*-dependent control of *ETH* gene expression.

We predict that CRC controls *ETH* transcription by binding to regulatory sequences directly upstream of the *ETH* promoter. To identify potential CRC recognition elements, we obtained a comparative genome alignment of a 404 bp sequence extending from immediately 3′ of the stop codon in the *Origin recognition complex subunit 4* (*Orc4*) gene through the first 10 bp of the *ETH* coding sequence (Fig. 7). This region contains the 382 bp *ETH* promoter region used to create the *ETH-EGFP* line (Park et al., 2002). In pairwise VISTA alignments of the sequence from *D. melanogaster* with the corresponding sequences from five other *Drosophila* species (*pseudoobscura*, *yakuba*, *ananassae*, *mojavensis*, and *virilis*), we detected three highly conserved regions (Fig. 7A). One was centered on the translational start site, and the other two conserved regions (CR1 and CR2) were located 91–171 bp upstream of the *ETH* translational start site [77–157 bp upstream of the predicted transcriptional start site (Park et al., 1999)].

Using MAVID, we added the corresponding sequences from two additional species, *D. erecta* and *D. simulans*, to the alignment. Based on these eight genomes, we obtained a *Drosophila* genus consensus sequence for CR1 and CR2 (Fig. 7B). An rVISTA analysis to detect putative ATF-4 binding sites resulted in three matches, at the same position in each species, in the aligned *D. yakuba*, *D. pseudoobscura*, *D. ananassae*, *D. mojavensis* and *D. virilis* sequences. One was located within the most conserved portion of CR1, a second was found in CR2, and the third was located 21 nucleotides upstream of the *ETH* translational start site. In *D. yakuba*, all three hits were conserved [at least 80% identical over a 24 bp window (Loots et al., 2002)], and the CR2 hit was conserved in *D. pseudoobscura*. The other hits in *D. pseudoobscura* and in the other three species did not meet the 80% conservation threshold. In addition to these matches, we

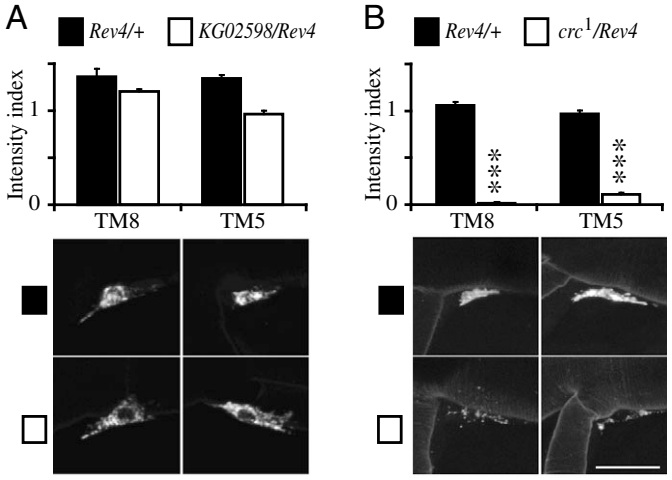

Fig. 6. Reduced *ETH* reporter gene expression in *crc* mutant third instar larvae. Expression of EGFP was driven under the control of a 382 bp promoter sequence from the *ETH* gene. (A,B) Intensity of Inka cell (TM5 and TM8) EGFP fluorescence in (A) *Rev4, ETH-EGFP/*$dimm^{KG02598}$ (*N*=9) *vs Rev4, ETH-EGFP/+* (*N*=4) and (B) *Rev4, ETH-EGFP/*crc^1 (*N*=9) *vs Rev4, ETH-EGFP/+* (*N*=11) larvae. ****P*<0.001; one-way ANOVA. Scale bar, 5 μm.

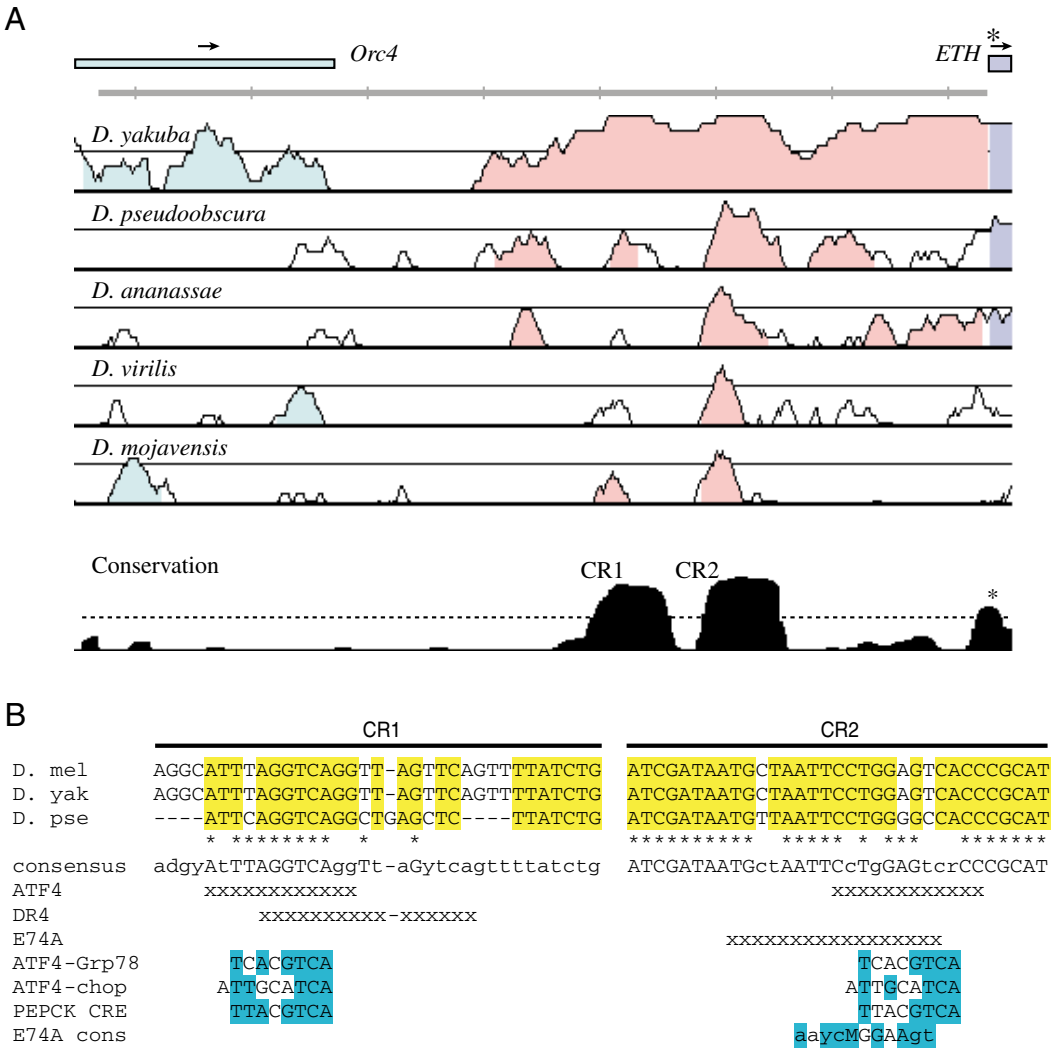

Fig. 7. Comparative genomic analysis of the 382 bp *ETH* gene regulatory region. (A) VISTA plot of the *D. melanogaster* assembly in pairwise alignments with five other *Drosophila* species. The gray bar, with tick marks at 50 bp intervals, shows the extent of the 382 bp region. The percent identity from 50–100% (vertical axis) in a 20 bp window sliding in 1 bp increments is displayed for each alignment (horizontal axis). Windows (excluding gaps) that were at least 70% identical with *D. melanogaster* are highlighted (non-coding sequences in pink). The conservation track (bottom plot) shows phastCons scores for the three-way MULTIZ alignment of *D. melanogaster*, *D. yakuba* and *D. pseudoobscura*. Two highly conserved regions (CR1 and CR2) exceeded the 0.4 score threshold (broken line). Arrows, direction of transcription; asterisks, start ATG of the *ETH* gene [the 5′ UTR of *ETH* is predicted to be 14 bp long (Park et al., 1999)]; purple box, *ETH* coding sequence; turquoise box, *Orc4* 3′ UTR. (B) MULTIZ alignment of CR1 and CR2. Bases that were identical in at least seven *Drosophila* species are indicated with asterisks with the consensus sequence shown directly below. Positions marked x below the consensus denote ATF4, DR4 and E74A binding sites predicted by rVISTA. Four selected transcription factor binding sites (see Results) are also shown at the bottom of the alignment, and bases matching the CR1 or CR2 consensus are highlighted in blue.

also obtained one conserved hit in CR2 in *D. yakuba* and *D. pseudoobscura* for the TRANSFAC consensus binding sequence for *Drosophila* transcription factors encoded by the *E74* early ecdysone-inducible gene (*Eip74EF*) (Fig. 7B). This sequence was an imperfect match to a consensus binding site for E74A determined by random oligonucleotide selection (E74A cons) (Urness and Thummel, 1990). Finally, the conserved portion of CR1 also contains a putative ecdysteroid response element (DR4), which consists of an imperfect direct repeat of AGGTCA separated by 4 nucleotides (Park et al., 1999). This sequence was also a conserved hit (with the DR4 consensus) in our rVISTA analysis of the *D. yakuba* and *D. pseudoobscura* sequences (data not shown).

We compared the *Drosophila* genus consensus sequence for the predicted ATF-4 sites in CR1 and CR2 to the ATF-4 binding site in the rat *Grp78* promoter (ATF4-Grp78) (Luo et al., 2003), the CAATT-enhancer binding protein (C/EBP)-activating transcription factor (ATF) composite site in the hamster *chop* promoter (ATF4-chop) (Fawcett et al., 1999; Ma et al., 2002), and the cAMP response element (CRE) in the rat

phoshpenolpyruvate carboxykinase (*PEPCK*) gene (PEPCK CRE) (Vallejo et al., 1993) (Fig. 7B). All of these confirmed ATF-4-binding sites were imperfect matches to the ATF4 rVISTA hits in the *Drosophila* sequences. The best match (7 of 8 nucleotides) was between the CR1 hit and the *PEPCK* CRE. The latter has been shown to bind ATF-4-C/EBPβ heterodimers (Vallejo et al., 1993). Thus, there is strong conservation of two sequences in the *ETH* promoter that are close, but imperfect matches to known binding sites for ATF-4, the mammalian ortholog of CRC. We predict that one or both of these putative CRC binding sites is required for CRC-dependent expression of *ETH*.

Discussion

dimm controls levels of Lk, Fmrf and Dms neuropeptide mRNAs

DIMM has been proposed as a direct regulator of neuroendocrine gene expression in most neuropeptidergic cells (Allan et al., 2005; Hewes et al., 2003). Here we present qRTPCR results, supplemented by *in situ* hybridization, showing that DIMM upregulates the levels of mRNAs derived from at least three neuropeptide genes, *Fmrf*, *Lk* and *Dms*. These findings provide strong support for DIMM as a key regulator of multiple neuroendocrine genes.

The LIM-homeodomain gene *apterous* (*ap*) also controls *Fmrf* and *Lk* gene expression (Allan et al., 2005; Allan et al., 2003; Benveniste et al., 1998; Herrero et al., 2003; Park et al., 2004). *ap* acts cell-autonomously to stimulate *dimm* expression, but the AP and DIMM proteins can also physically interact, and they may function together in regulating *Fmrf* (Allan et al., 2005). Several other factors, including the transcriptional co-factors encoded by *dachshund* and *eyes absent* (Miguel-Aliaga et al., 2004), the zinc-finger gene *squeeze*, and the retrograde bone morphogenetic protein (BMP) pathway, act in combinatorial fashion with *dimm* and *ap* to control *Fmrf* expression (Allan et al., 2005; Allan et al., 2003). However, other neuropeptidergic cells appear to use only portions of this code. For example, *ap* and *dimm* appear to contribute to the expression of *Lk* in *Fmrf*-negative cells (A1–A7 and possibly Br1). Even within the population of *Lk* cells, loss of *dimm* results in very different effects in different neurons, with a reduction in *Lk* transcript levels in cells A1–A7, and an increase (or no change) in *Lk* levels in the Br1 and SE neurons (Fig. 4). How do these relatively widely expressed factors interact with other regulatory proteins to produce cell type-specific patterns of neuropeptide gene expression? It will be of interest to determine which other elements of the combinatorial pro-*Fmrf* code are used to control *Lk* and *Dms* expression, and to identify additional factors that interact with *dimm* to control expression of these neuropeptide genes.

Does dimm control neuropeptide levels through an additional indirect mechanism?

We did not detect changes in levels of three neuropeptide biosynthetic enzyme mRNAs, *Phm*, *Fur1* and *amon*, in the qRTPCR analysis. This is in contrast to our earlier immunocytochemical studies, in which we observed a marked reduction in the protein products of these genes in *dimm* mutant CNS (Hewes et al., 2003). In some cases, these differences may reflect the spatial insensitivity of the qRTPCR methods, as was confirmed by our *in situ* hybridization analysis of *Lk* expression (Fig. 4). *Phm*, in particular, may belong in this category. Although levels of PHM and DIMM expression are strongly correlated (Allan et al., 2005; Hewes et al., 2003), PHM is also highly expressed in many other tissues (Jiang et al., 2000) that do not express *dimm*. Any *dimm*-dependent change in *Phm* expression may have been obscured by the much larger pool of *dimm*-independent *Phm* mRNA in our whole-animal qRTPCR analysis.

DIMM may regulate levels of other neuroendocrine proteins through a route that does not involve interactions between DIMM and *cis*-regulatory elements in the respective genes. We obtained the first evidence in support of this hypothesis in our earlier analysis of an ectopically expressed neuropeptide in *dimm* mutant cells; levels of ectopic PDF protein were strongly reduced while *dimm* had no effect on levels of the cognate *Pdf* mRNA (Hewes et al., 2003). Here, we show that larvae homozygous for a specific loss-of-function mutation in *dimm* displayed reduced levels of endogenous ETH-like protein(s), but not *ETH* mRNA, in the endocrine Inka cells (see Fig. S1 in the supplementary material), a site of *dimm* gene expression (Hewes et al., 2003). This may occur simply through a *dimm*-dependent change in levels of one secreted protein, such as PHM, that may disrupt the formation of multi-protein aggregates required for neuropeptide sorting into secretory granules (Arvan and Castle, 1998; Brakch et al., 2002). Alternatively, recent studies on the mouse ortholog of *dimm*, *Mist1*, suggest that *dimm* may play a more direct role in the management of secretory granule budding from the trans-Golgi network. In *Mist1* knockout mice ($Mist1^{KO}$), pancreatic exocrine cells display reduced intracellular organization (Pin et al., 2001). Moreover, the $Mist1^{KO}$ phenotype is partially phenocopied in animals mutant for the *Rab3D* gene, a small GTPase involved in secretory granule trafficking (Johnson et al., 2004). Further studies on the regulation of ETH, PHM and Rab3-like proteins, and on the biochemical interactions among them, may shed light on the cellular mechanisms underlying the indirect actions of DIMM.

crc controls expression of ETH through a 382 bp 5′ region

Mutations in the *crc* gene result in pleiotropic defects in ecdysone-regulated events during molting and metamorphosis (Hewes et al., 2000). Many of the morphological defects are associated with a failure of the insect to properly complete ecdysis, a stereotyped set of behaviors required for shedding of the old cuticle at the culmination of each molt. Several neuropeptides and peptide hormones, including ETH, play critical roles in organizing and triggering ecdysis behavior (Ewer and Reynolds, 2002).

Here we provide four independent lines of evidence that demonstrate a crucial role for *crc* in the upregulation of *ETH*

mRNA levels. First, we observed a marked reduction by qRTPCR in levels of *ETH* transcripts [but not in mRNAs encoding CCAP or EH, two other neuropeptides involved in the neuropeptide hierarchy controlling ecdysis (Ewer and Reynolds, 2002)] in *crc* mutant larvae (Fig. 2). Second, *in situ* hybridization revealed a strong reduction in *ETH* mRNA levels in the endocrine Inka cells in *crc* mutant larvae (Fig. 5). Third, the intensity of anti-PETH immunoreactivity was markedly reduced in crc^1/crc^1 homozygotes. Fourth, EGFP fluorescence driven by an *ETH-EGFP* reporter gene was reduced in *crc* mutant larvae (Fig. 6). Therefore, CRC is a strong activator of *ETH* gene expression, and loss of CRC results in a corresponding reduction in levels of the ETH protein.

Despite the molecular identification of the *crc* locus (Hewes et al., 2000), almost six decades after the original description of the first *crc* allele (Hadorn and Gloor, 1943), the causes of the molting and metamorphosis defects in *crc* mutants remained unclear. Our current results suggest a simple model to explain the *crc* mutant phenotype. Strong hypomorphic or null mutations in *crc* and *ETH* both severely disrupt ecdysis. These defects include weak, irregular and slower ecdysis contractions and a failure to shed old cuticular structures, leading to retention of two and sometimes three sets of mouthparts into the next larval stage (Chadfield and Sparrow, 1985; Park et al., 2002). These similarities in molting defects, taken together with our observation that *crc* is required for normal expression of *ETH* mRNA and ETH protein, point to the loss of ETH signaling as the likely proximate cause of the ecdysis defects observed in *crc* mutants.

Despite the specific effects of *crc* on *ETH* transcription in the Inka cells, *crc* is widely expressed (Hewes et al., 2000), suggesting a cellular housekeeping function. The vertebrate ATF-4 protein is also ubiquitously expressed (Hai and Hartman, 2001). In addition, the upregulation of *ATF-4* constitutes a milestone of many cellular stress response pathways including oxidative stress, amino acid deprivation (Rutkowski and Kaufman, 2003), and hypoxia (Blais et al., 2004). In the tobacco hornworm, *Manduca sexta*, levels of ETH fluctuate during the molts and are regulated by circulating ecdysteroids (Zitnan et al., 1999). We hypothesize that CRC contributes to the regulation of *ETH* gene expression during this period, perhaps in response to signals from the tracheae.

Predicted CRC binding sites in the ETH *promoter region*

Peaks in circulating levels of the ecdysteroid hormone, 20-hydroxyecdysone (20HE), initiate and coordinate each molt. A subsequent decline in 20HE levels is required for ecdysis, and the activation of these behaviors involves a hierarchical cascade of peptide hormone and neuropeptide signals that is triggered by ETH (Ewer and Reynolds, 2002). Is CRC required in order to maintain ETH expression, or is CRC involved in regulating transcription of the *ETH* gene during the molts? While it is not known whether *ETH* mRNA levels fluctuate during *Drosophila* post-embryonic development, the regulation of ETH levels by ecdysteroids in molting *Manduca sexta*, and our analysis of the CR1 and CR2 sequences, provides tantalizing clues to possible coordinate regulation of *ETH* gene expression by CRC and ecdysone response genes. There is substantial overlap between the predicted CRC binding site in CR1 and a putative ecdysteroid response element (EcRE) (cf. Park et al., 1999). In addition, we found a potential binding site in CR2 for products of the *E74* early ecdysone-inducible gene. *E74* expression is induced directly by 20HE, and it encodes transcription factors that regulate other ecdysone response genes (Fletcher and Thummel, 1995). Mutations that specifically disrupt E74B, which likely binds the same consensus as E74A (Urness and Thummel, 1990), display defects associated with pupal ecdysis that closely phenocopy *crc*. In future studies we hope to determine if *ETH* expression is regulated by elements in both CR1 and CR2 in an ecdysteroid-dependent manner, and whether CRC, E74B and other factors in the ecdysone-response pathway interact competitively or cooperatively at these sites.

List of abbreviations

20HE	20-hydroxyecdysone
amon	*amontillado*
ap	*apterous*
ATF-4	activating transcription factor-4
B	background
bHLH	basic helix-loop-helix
BMP	bone morphogenetic protein
bZIP	basic-leucine zipper
C/EBP	CAATT-enhancer binding protein
Caps	*Calcium activated protein for secretion*
Ccap	*Cardioacceleratory peptide*
CNS	central nervous system
CR	*ETH* promoter conserved region
crc	*cryptocephal*
CRE	cAMP response element
Ct	cycles to threshold amplicon concentration
Ddc	*Dopa decarboxylase*
dimm	*dimmed*
Dms	*Dromyosuppressin*
Dsk	*Drososulfakinin*
EcRE	ecdysteroid response element
EGFP	enhanced green-fluorescent protein
Eh	*Eclosion hormone*
Eip74EF (*E74*)	*Ecdysone-induced protein 74EF*
ETH	*Ecdysis triggering hormone*
Fmrf	FMRFamide-related
Fur1	*Furin 1*
Lk	*Leucokinin*
NoE	No Enzyme
NoT	No Template
Orc4	*Origin recognition complex subunit 4*
Pdf	*Pigment–dispersing factor*
PEPCK	*phospenolpyruvate carboxykinase*
PETH	pre-ecdysis triggering hormone
Phm	*Peptidylglycine-α-hydroxylating*

	monooxygenase
ple	*pale*
qRTPCR	quantitative real time polymerase chain reaction
RpL32 (rp49)	*Ribosomal protein L32*
S	soma
TM	tracheal metamere
T_m	melting temperature
Tsp39D	*Tetraspanin 39D*
VNC	ventral nerve cord
y	*yellow*

We thank Chad Hargrave for statistical guidance, Mike Adams for fly stocks and antisera, David Durica for comments on the manuscript, and Audrey Kennedy, Kendal Milam, Matthew Mote, Jeremiah Smith and Elizabeth Pearsall for technical assistance. This work was supported by grants from the National Science Foundation (NSF IBN0344018), NSF EPSCoR and the Oklahoma State Regents for Higher Education (NSF-0132534), and the Oklahoma Center for the Advancement of Science and Technology (HR03-048S) to R.S.H.

References

Allan, D. W., Pierre, S. E., Miguel-Aliaga, I. and Thor, S. (2003). Specification of neuropeptide cell identity by the integration of retrograde BMP signaling and a combinatorial transcription factor code. *Cell* **113**, 73-86.

Allan, D. W., Park, D., St Pierre, S. E., Taghert, P. H. and Thor, S. (2005). Regulators acting in combinatorial codes also act independently in single differentiating neurons. *Neuron* **45**, 689-700.

Arvan, P. and Castle, D. (1998). Sorting and storage during secretory granule biogenesis: looking backward and looking forward. *Biochem. J.* **332**, 593-610.

Bellen, H. J., Levis, R. W., Liao, G., He, Y., Carlson, J. W., Tsang, G., Evans-Holm, M., Hiesinger, P. R., Schulze, K. L., Rubin, G. M. et al. (2004). The BDGP gene disruption project: single transposon insertions associated with 40% of *Drosophila* genes. *Genetics* **167**, 761-781.

Benveniste, R. J., Thor, S., Thomas, J. B. and Taghert, P. H. (1998). Cell type-specific regulation of the *Drosophila FMRF-NH2* neuropeptide gene by Apterous, a LIM homeodomain transcription factor. *Development* **125**, 4757-4765.

Blais, J. D., Filipenko, V., Bi, M., Harding, H. P., Ron, D., Koumenis, C., Wouters, B. G. and Bell, J. C. (2004). Activating transcription factor 4 is translationally regulated by hypoxic stress. *Mol. Cell Biol.* **24**, 7469-7482.

Brakch, N., Allemandou, F., Cavadas, C., Grouzmann, E. and Brunner, H. R. (2002). Dibasic cleavage site is required for sorting to the regulated secretory pathway for both pro- and neuropeptide Y. *J. Neurochem.* **81**, 1166-1175.

Bray, N. and Pachter, L. (2004). MAVID: constrained ancestral alignment of multiple sequences. *Genome Res.* **14**, 693-699.

Burbach, J. P. (2002). Regulation of gene promoters of hypothalamic peptides. *Front. Neuroendocrinol.* **23**, 342-369.

Cavener, D. R. (1987). Comparison of the consensus sequence flanking translational start sites in *Drosophila* and vertebrates. *Nucleic Acids Res.* **15**, 1353-1361.

Celniker, S. E., Wheeler, D. A., Kronmiller, B., Carlson, J. W., Halpern, A., Patel, S., Adams, M., Champe, M., Dugan, S. P., Frise, E. et al. (2002). Finishing a whole-genome shotgun: release 3 of the *Drosophila melanogaster* euchromatic genome sequence. *Genome Biol.* **3**, RESEARCH0079.1-RESEARCH0079.14.

Chadfield, C. G. and Sparrow, J. C. (1985). Pupation in *Drosophila melanogaster* and the effect of the *lethalcryptocephal* mutation. *Dev. Genet.* **5**, 103-114.

Ewer, J. and Reynolds, S. E. (2002). Neuropeptide control of molting in insects. In *Hormones, Brain and Behavior in Invertebrates.* Vol. 3 (ed. D. W. Pfaff, A. P. Arnold, A. M. Etgen, S. E. Fahrbach and R. T. Rubin), pp. 1-92. New York: Academic Press.

Fawcett, T. W., Martindale, J. L., Guyton, K. Z., Hai, T. and Holbrook, N. J. (1999). Complexes containing activating transcription factor (ATF)/cAMP-responsive-element-binding protein (CREB) interact with the CCAAT/enhancer-binding protein (C/EBP)-ATF composite site to regulate *Gadd153* expression during the stress response. *Biochem. J.* **339**, 135-141.

Fletcher, J. C. and Thummel, C. S. (1995). The ecdysone-inducible *Broad-complex* and *E74* early genes interact to regulate target gene transcription and *Drosophila* metamorphosis. *Genetics* **141**, 1025-1035.

Frazer, K. A., Pachter, L., Poliakov, A., Rubin, E. M. and Dubchak, I. (2004). VISTA: computational tools for comparative genomics. *Nucleic Acids Res.* **32**, W273-W279.

Hadorn, E. and Gloor, H. (1943). *Cryptocephal* ein spat wirkender Letalfaktor bei *Drosophila melanogaster*. *Rev. Suisse Zool.* **50**, 256-261.

Hai, T. and Hartman, M. G. (2001). The molecular biology and nomenclature of the activating transcription factor/cAMP responsive element binding family of transcription factors: activating transcription factor proteins and homeostasis. *Gene* **273**, 1-11.

Hassan, B. A. and Bellen, H. J. (2000). Doing the MATH: is the mouse a good model for fly development? *Genes Dev.* **14**, 1852-1865.

Herrero, P., Magarinos, M., Torroja, L. and Canal, I. (2003). Neurosecretory identity conferred by the *apterous* gene: lateral horn leucokinin neurons in *Drosophila*. *J. Comp. Neurol.* **457**, 123-132.

Hewes, R. S. and Taghert, P. H. (2001). Neuropeptides and neuropeptide receptors in the *Drosophila melanogaster* genome. *Genome Res.* **11**, 1126-1142.

Hewes, R. S., Schaefer, A. M. and Taghert, P. H. (2000). The *cryptocephal* gene (ATF4) encodes multiple basic-leucine zipper proteins controlling molting and metamorphosis in *Drosophila*. *Genetics* **155**, 1711-1723.

Hewes, R. S., Park, D., Gauthier, S. A., Schaefer, A. M. and Taghert, P. H. (2003). The bHLH protein Dimmed controls neuroendocrine cell differentiation in *Drosophila*. *Development* **130**, 1771-1781.

Jiang, N., Kolhekar, A. S., Jacobs, P. S., Mains, R. E., Eipper, B. A. and Taghert, P. H. (2000). PHM is required for normal developmental transitions and for biosynthesis of secretory peptides in *Drosophila*. *Dev. Biol.* **226**, 118-136.

Johnson, C. L., Kowalik, A. S., Rajakumar, N. and Pin, C. L. (2004). Mist1 is necessary for the establishment of granule organization in serous exocrine cells of the gastrointestinal tract. *Mech. Dev.* **121**, 261-272.

Karolchik, D., Baertsch, R., Diekhans, M., Furey, T. S., Hinrichs, A., Lu, Y. T., Roskin, K. M., Schwartz, M., Sugnet, C. W., Thomas, D. J. et al. (2003). The UCSC Genome Browser Database. *Nucleic Acids Res.* **31**, 51-54.

Livingstone, M. S. and Tempel, B. L. (1983). Genetic dissection of monoamine neurotransmitter synthesis in *Drosophila*. *Nature* **303**, 67-70.

Loots, G. G., Ovcharenko, I., Pachter, L., Dubchak, I. and Rubin, E. M. (2002). rVista for comparative sequence-based discovery of functional transcription factor binding sites. *Genome Res.* **12**, 832-839.

Luo, S., Baumeister, P., Yang, S., Abcouwer, S. F. and Lee, A. S. (2003). Induction of Grp78/BiP by translational block: activation of the *Grp78* promoter by ATF4 through and upstream ATF/CRE site independent of the endoplasmic reticulum stress elements. *J. Biol. Chem.* **278**, 37375-37385.

Ma, Y., Brewer, J. W., Diehl, J. A. and Hendershot, L. M. (2002). Two distinct stress signaling pathways converge upon the CHOP promoter during the mammalian unfolded protein response. *J. Mol. Biol.* **318**, 1351-1365.

Manning, G. and Krasnow, M. A. (1993). Development of the *Drosophila* tracheal system. In *The Development of Drosophila melanogaster* (ed. A. Martinez-Arias and M. Bate), pp. 609-668. Cold Spring Harbor: Cold Spring Harbor Press.

Miguel-Aliaga, I., Allan, D. W. and Thor, S. (2004). Independent roles of the *dachshund* and *eyes absent* genes in BMP signaling, axon pathfinding and neuronal specification. *Development* **131**, 5837-5848.

Nässel, D. R. (2002). Neuropeptides in the nervous system of *Drosophila* and other insects: multiple roles as neuromodulators and neurohormones. *Prog. Neurobiol.* **68**, 1-84.

Neckameyer, W. S. and White, K. (1993). *Drosophila* tyrosine hydroxylase is encoded by the *pale* locus. *J. Neurogenet.* **8**, 189-199.

Nichols, R. (2003). Signaling pathways and physiological functions of *Drosophila melanogaster* FMRFamide-related peptides. *Annu. Rev. Entomol.* **48**, 485-503.

Nichols, R., McCormick, J. and Lim, I. (1997). Multiple antigenic peptides designed to structurally related *Drosophila* peptides. *Peptides* **18**, 41-45.

O'Brien, M. A. and Taghert, P. H. (1998). A peritracheal neuropeptide system in insects: release of myomodulin-like peptides at ecdysis. *J. Exp. Biol.* **201**, 193-209.

O'Connell, P. O. and Rosbash, M. (1984). Sequence, structure, and codon preference of the *Drosophila ribosomal protein 49* gene. *Nucleic Acids Res.* **12**, 5495-5513.

Park, D., Han, M., Kim, Y. C., Han, K. A. and Taghert, P. H. (2004). Aplet neurons – a peptidergic circuit potentially controlling ecdysial behavior in *Drosophila*. *Dev. Biol.* **269**, 95-108.

Park, Y., Zitnan, D., Gill, S. S. and Adams, M. E. (1999). Molecular cloning and biological activity of ecdysis-triggering hormones in *Drosophila melanogaster*. *FEBS Lett.* **463**, 133-138.

Park, Y., Filippov, V., Gill, S. S. and Adams, M. E. (2002). Deletion of the *ecdysis-triggering hormone* gene leads to lethal ecdysis deficiency. *Development* **129**, 493-503.

Pin, C. L., Rukstalis, J. M., Johnson, C. and Konieczny, S. F. (2001). The bHLH transcription factor Mist1 is required to maintain exocrine pancreas cell organization and acinar cell identity. *J. Cell Biol.* **155**, 519-530.

Renden, R., Berwin, B., Davis, W., Ann, K., Chin, C. T., Kreber, R., Ganetzky, B., Martin, T. F. and Broadie, K. (2001). *Drosophila* CAPS is an essential gene that regulates dense-core vesicle release and synaptic vesicle fusion. *Neuron* **31**, 421-437.

Rice, W. (1989). Analyzing tables of statistical tests. *Evolution* **43**, 223-225.

Richards, S., Liu, Y., Bettencourt, B. R., Hradecky, P., Letovsky, S., Nielsen, R., Thornton, K., Hubisz, M. J., Chen, R., Meisel, R. P. et al. (2005). Comparative genome sequencing of *Drosophila pseudoobscura*: chromosomal, gene, and *cis*-element evolution. *Genome Res.* **15**, 1-18.

Roebroek, A. J., Pauli, I. G., Zhang, Y. and van de Ven, W. J. (1991). cDNA sequence of a *Drosophila melanogaster* gene, *Dfur1*, encoding a protein structurally related to the subtilisin-like proprotein processing enzyme furin. *FEBS Lett.* **289**, 133-137.

Roseman, R. R., Johnson, E. A., Rodesch, C. K., Bjerke, M., Nagoshi, R. N. and Geyer, P. K. (1995). A *P* element containing *suppressor of hairy-wing* binding regions has novel properties for mutagenesis in *Drosophila melanogaster*. *Genetics* **141**, 1061-1074.

Rozen, S. and Skaletsky, H. (2000). Primer3 on the WWW for general users and for biologist programmers. *Methods Mol. Biol.* **132**, 365-386.

Rutkowski, D. T. and Kaufman, R. J. (2003). All roads lead to ATF4. *Dev. Cell* **4**, 442-444.

SantaLucia, J., Jr (1998). A unified view of polymer, dumbbell, and oligonucleotide DNA nearest-neighbor thermodynamics. *Proc. Natl. Acad. Sci. USA* **95**, 1460-1465.

Schneider, L. E., O'Brien, M. A. and Taghert, P. H. (1991). In situ hybridization analysis of the FMRFamide neuropeptide gene in Drosophila. I. Restricted expression in embryonic and larval stages. *J. Comp. Neurol.* **304**, 608-622.

Siekhaus, D. E. and Fuller, R. S. (1999). A role for *amontillado*, the *Drosophila* homolog of the neuropeptide precursor processing protease PC2, in triggering hatching behavior. *J. Neurosci.* **19**, 6942-6954.

Siepel, A. and Haussler, D. (2005). Phylogenetic hidden Markov models. In *Statistical Methods in Molecular Evolution* (ed. R. Nielsen), pp. 325-351. New York: Springer.

Strand, F. L. (1999). *Neuropeptides: Regulators of Physiological Processes*. Cambridge, MA: MIT Press.

Taghert, P. H. (1999). FMRFamide neuropeptides and neuropeptide-associated enzymes in *Drosophila*. *Microsc. Res. Tech.* **45**, 80-95.

Todres, E., Nardi, J. B. and Robertson, H. M. (2000). The tetraspanin superfamily in insects. *Insect Mol. Biol.* **9**, 581-590.

Urness, L. D. and Thummel, C. S. (1990). Molecular interactions within the ecdysone regulatory hierarchy: DNA binding properties of the *Drosophila* ecdysone-inducible E74A protein. *Cell* **63**, 47-61.

Vallejo, M., Ron, D., Miller, C. P. and Habener, J. F. (1993). C/ATF, a member of the activating transcription factor family of DNA-binding proteins, dimerizes with CAAT/enhancer-binding proteins and directs their binding to cAMP response elements. *Proc. Natl. Acad. Sci. USA* **90**, 4679-4683.

Vanden Broeck, J. (2001). Neuropeptides and their precursors in the fruitfly, *Drosophila melanogaster*. *Peptides* **22**, 241-254.

Walchli, S., Colinge, J. and Hooft van Huijsduijnen, R. (2000). MetaBlasts: tracing protein tyrosine phosphatase gene family roots from Man to *Drosophila melanogaster* and *Caenorhabditis elegans* genomes. *Gene* **253**, 137-143.

Zitnan, D., Ross, L. S., Zitnanova, I., Hermesman, J. L., Gill, S. S. and Adams, M. E. (1999). Steroid induction of a peptide hormone gene leads to orchestration of a defined behavioral sequence. *Neuron* **23**, 523-535.

Zitnan, D., Zitnanova, I., Spalovska, I., Takac, P., Park, Y. and Adams, M. E. (2003). Conservation of ecdysis-triggering hormone signalling in insects. *J. Exp. Biol.* **206**, 1275-1289.

Table S1. *Optimal primers obtained for qRTPCR and in situ hybridization*

Primer	Primer sequence (5′ to 3′)	Amplicon length (nt)	Amplicon T_m during qRTPCR (°C)	Primer concentration (nmol l^{-1})
amon forward	aggtcaggtccagataaaca	108	80	750
amon reverse	aaataaaacacagccagcac			500
Caps forward	tggaaactagacgctctacaa	110	78	550
Caps reverse	tctatcatatccactgccatc			600
Ccap forward	tacaatggaagtacgagaagc	101	81	850
Ccap reverse	gcgtttgaatagcgagaat			450
crc forward	ctgtctaaagaaaacgagcag	94	84	850
crc reverse	catggtagaactctcgaatca			500
Ddc forward	gccacatacccattagtaaca	110	77	650
Ddc reverse	acccaatagacataccgaaac			500
dimm forward	gatgcacagcctaaacga	103	82	350
dimm reverse	tttggccagtgtgagtgt			300
Dms forward[a]	atgtcgatcacgtcttcct	103	81	415
Dms reverse[a]	cagtgtcgttgtctcatgtc			525
Dsk forward	gtctacagaacgctaaggatg	105	78	1050
Dsk reverse	gagagaatgatggtccaactaa			400
Eh forward	tagtcagctccccaaaca	99	79	500
Eh reverse	attgcaactgccacaaag			375
ETH forward[a]	atgggatttggaaacgag	109	84	350
ETH reverse[a]	aaggagcgtattcgagttg			450
Fmrf forward	ttacgcccagaacaaataag	110	79	500
Fmrf reverse	ttgaagtgggtagacaacaa			950
Fur1 forward	tagcaacaccactaacagca	110	80	450
Fur1 reverse	cagcatttgaccctaattgt			575
ia2 forward	gggtcttttcagttcgtatagt	90	78	1250
ia2 reverse	caatctcgtgaagcctttt			450
Lk forward[a]	atgaacctgcggtacttg	108	84	725
Lk reverse[a]	ctttggccgtcaagtctat			500
Pdf forward	tgatcctcgagaactcctt	101	83	625
Pdf reverse	cgcatcgttcatgttctt			375
Phm forward	cttccaaacaggaaggtttt	90	78	400
Phm reverse	gtggcattttcaccgtatt			360
ple forward	acaacccaaacacacaaaac	106	80	375
ple reverse	gatggatagccattctcaatac			600
RpL32 forward	gatccgtaaccgatgttg	100	83	650
RpL32 reverse	ctaagctgtcgcacaaatg			425
Tsp39D forward	tcgttagcgatcacgtct	104	81	450
Tsp39D reverse	gctctcttttaaggctccac			400

[a]Primers used for preparation of *in situ* probes: *Lk*, 5′-gatagtcctgtgtatggtgct-3′ and 5′-gacttcaactttggctgttc-3′; *Dms*, 5′-caactctgatgacctgttga-3′ and 5′-aacggaaaatagtgtttgga-3′; *ETH*, 5′-gcacagctctgttactcctc-3′ and 5′-cgaatactccacatctcacag-3′.

Table S2. *Complementation analysis of* $dimm^{EY14636}$

dimm class	*crc* class	Allele	*N*	% Cy^+ expected
Null	Null	*Rev4*	114	11***
Hypomorph	Null	*Rev8*	114	25***
Hypomorph	Weak hypomorph	$dimm^{KG02598}$	165	59**
+	Severe hypomorph	crc^1	352	91

Each allele was crossed to $dimm^{EY14636}$. crc^1 was balanced over *CyO*-y^+. The other alleles were balanced over *CyO, Ubi-GFP*, and all mutations were maintained in a *y* w** background.

***P*<0.01, ****P*<0.001 (χ^2 test).